Assessment of combined wind and wave energy in the tropical cyclone affected region：An application in China seas

Jiangxia Li[a,b], Shunqi Pan[c], Yongping Chen[d,e], Yu Yao[a,b,*], Conghao Xu[a,b]

a School of Hydraulic Engineering, Changsha University of Science and Technology, Changsha, 410114, China

b Key Laboratory of Water-Sediment Sciences and Water Disaster Prevention of Hunan Province, Changsha, 410114, China

c Hydro-environmental Research Centre, School of Engineering, Cardiff University, Cardiff, CF24 3AA, United Kingdom

d State Key Laboratory of Hydrology-Water Resources and Hydraulic Engineering, Hohai University, Nanjing, 210098, China

e College of Harbour, Coastal and Offshore Engineering, Hohai University, Nanjing, 210098, China

Abstract

Marine renewable energy resources are important for clean energy development. Research on the combined assessment of wind and wave resources, especially in tropical cyclone (TC) affected area is still rare. This study is to assess the potential combined wind and wave energy in the coastal waters of China, where TCs frequently occurred. The study utilizes the blended wind field with a parametric TC model based on the ECMWF reanalysis wind data from 1979 to 2013 for assessing potential wind energy, and the waves generated by the same wind data using the FVCOM-SWAVE model for assessing wave energy. The combined wind and wave energy density and annual power generation are analyzed. The potential energy from wind and waves at 15 nearshore locations along China east coasts are estimated. The results show that the frequency and intensity of TCs have a considerable impact on the distribution of density and stability of wind and wave energy, especially in the southeastern coastal areas of China. Suggestions of site selection of co-located wind and wave farm in the coastal waters of China are given. The research outcome provides a useful guidance for the selection of potential sites and design of wind and wave energy converters along the China coasts.

Keywords: wind energy; wave energy; tropical cyclone; China seas

1. Introduction

Renewable energy resources have been attracting attentions in clean energy development because of the finite supply of fossil fuels and the protection of the environment. There are many types of renewable energy resources such as solar, wind, and ocean (i.e., waves, tides, and currents) energy [1]. Being among the impressive list of renewable energy resources and as a promising alternative to fossil fuels, offshore wind and wave energy provides an effective means to solve our energy and environmental issues.

According to the results of the Third Nationwide Survey of Wind Energy Resources organized by the China Meteorological Administration in 2004-2005[2], China has one of the world's largest wind resources, with a total exploitable wind energy resource of about 4350 GW, of which about 1000 GW onshore and 200 GW offshore can be commercially developed with currently existing technologies. Besides, according to the estimation of the State Oceanic Administration of China, about 128.5 GW of wave energy is technically available in the nearshore area of China, accounting for nearly a half of the electricity production in China [3]. Thus, the distribution and availability of the wind and wave energy in China's coastal waters become important and desirable for effective and sustainable exploitation and use in the future.

In China, the requirement for clean and renewable energy is becoming more urgent, as the world's largest emitter of greenhouse gases [4]. Usually, the research on the wind energy distributions in China is mostly focused on the onshore area [5-6]. Due to abundant renewable sources from the offshore wind and waves, the distribution of the wind energy resources in the coastal and offshore waters of China seas and methods to make use of them have been seen increasingly of the interest of many researchers [7-9]. The regional-scale wind resource assessment is aimed to obtain the technical wind energy potential which will be helpful for future offshore wind energy planning and the development of offshore wind turbines (WTs). For example, China Meteorological Administration (CMA) assessed

the wind energy potential over the Bohai Sea, the Yellow Sea and East China Sea based on the numerical model WERAS/CMA [10]. Hong et al. [11] studied the available offshore wind energy over the exclusive economic zone of China considering technical, spatial and economic constraints. Li et al. [12] investigated the wind speed and wind power over the Bohai Sea and the Yellow Sea focusing on the climatology, variability, and extreme climate. The results indicate that the daily mean wind speed is stronger (weaker) in winter (summer) season, with stronger (weaker) spatial variability. Decadal variances of the mean wind speed and the wind power are roughly within ±2% and ±5%, respectively, with a stronger variability along the southwestern coasts of the Yellow Sea. In the nearshore area, Nie and Li [13] investigated the technical potential of offshore wind energy over the sea area where the water depth is shallower than 250 m along China coast considering the influential factors including wind power density, water depth, wind turbine size, wind farm layout, and various spatial constraints.

Wave energy is also an important clean resource which could be exploited in the seas. In recent years, majority of the studies of wave energy in China's marine space are focused on the wave climate or the distribution of wave characters. Among them, numerical models are widely applied to obtain the required characteristics for wave analysis. Liang et al. [14] used the wind data generated from Weather Research and Forecasting (WRF) model in SWAN wave model and analyzed the spatial distribution of mean and largest significant wave height in the Bohai Sea, the Yellow Sea and, the East China Sea based on the 22-year long-term wave simulation results. Lv et al. [15] studied the annual and seasonal distributions of mean wave characteristics in the Bohai Sea using the 20-year wave hindcasting data. Li et al. [16,17] analyzed the distribution of mean and extreme waves in China Seas, as well as the nearshore areas along the China coast based on the 35-year numerical simulation results. Based on the wave hindcasting data modelled numerically, several studies have been identified to assess the wave energy resources in China seas. For example, Liang et al. [18] used the wave model SWAN to simulate wave parameters of the China East Adjacent Seas for a 22-year period and investigated the distribution of wave energy resources, and Wang et al. [19] assessed the wave energy in the Bohai Sea based on the 26-year wave hindcast data simulated by the same wave model. Observation data could also be

used. Wu et al. [20] evaluated the offshore wave energy resources in the East China Sea using the data obtained from six wave measurement buoys covering the period of 2011-2013.

The wind and wave energy assessments have been carried out in many places around the world from global scale [21-23] to regions in Europe [24-26], America [27], Canada [28] and Korea [29]. In general, the wind and wave are evaluated separately in those studies. As the wave condition is closely related to the local wind, it is worth studying the distribution of combined wind and wave energy together, which could provide a practical guidance for the design of integrated wind and wave energy converters and co-located wind-wave energy farms [30]. More recently, assessment of the combined wind and wave energy have been seen to arouse attention. Rusu et al. [31] conducted a parallel evaluation of wind and wave energy resources along the Latin American and European coast. Lira-Loarca et al. [32] assessed the future wind and wave energy resources in the Mediterranean Sea. Ferrari er al. [33] proposed an optimized method for combined assessment of wind and wave energy resources in the Mediterranean Sea. The correlation coefficient of wind and wave energy resources were analyzed, and the exploitation suggestions were given. Also, several studies about the layout of wind-wave farms are conducted [30,34]. In China, Wang et al. [35] assessed the wind and wave energy in the South China Sea based on 30-year hindcast data using WRF atmospheric model and WWIII wave model, focusing on the seasonal and monthly distribution. For a relatively large area, Zheng et al. [36-37] investigated wind energy and wave energy in the China seas and adjacent waters using long-term hindcast data. Wen et al. [38] conduct a joint study of offshore wind and wave energy along the south and southeast coast of China. Those studies are mainly focused on the distribution of wind and wave resources, the assessments on the relationship between wind and wave resources are rare. For a better arrangement of the wind, wave plant or the co-located wind-wave farm, the combined analysis on the wind and wave energy resources are required to be conducted.

Planning, designing and operating wind turbines (WTs) and wave energy converters (WECs) require a comprehensive understanding of the distribution of wind and wave energy potential for the interested area to make efficient use of the power [39]. After Lin et al. [40] assessed the wave energy in the China

adjacent seas on the basis of a 20-year SWAN simulation, they pointed out that the influence of TCs should be further considered as the wind speed near the TC centre from the reanalysis data are generally lower than the actual values. Tropical cyclones (TC), which have widely influence on the winds and waves around the world and always lead to extreme oceanic conditions, should be considered in the wind and wave energy assessment. Although rich in energy, the extremely large winds and waves during TC periods would hardly be utilized with a storm protection state mode be designed for the safety of energy converter device. In addition, ensuring the survivability of energy converter devices under the TC risks could be challenging and highly costly. For example, the OSPREY (Ocean Swell Powered Renewable EnergY) in UK and the Oscillation Water Column (OWC) plant in Portugal were destroyed in the severe sea conditions. The existing studies on the wind and wave energy distributions commonly use the reanalysis atmospheric data which may not accurately describe the TC wind conditions[41]. As the TC related studies on wind and wave resources are scarce, to guide the design of WTs and WECs, careful consideration of the wind and wave energy generated during TCs should be necessary when assessing the distribution of potential resources. Meanwhile, the China seas, located in the northwest Pacific Ocean, are frequently affected by TCs. To conduct the TC related assessment of wind and wave energy at these areas could be useful for relevant engineering projects.

In this study, a large-scale wave modelling framework is constructed which covers the entire coastal waters of China including the Bohai Sea, the Yellow Sea, the East China Sea and the north part of South China Sea (Fig. 1), in an attempt to assess the wind and wave energy density more accurately with the blended long-term wind forcing based on the ECMWF reanalysis wind data, but modified by the typhoon events through a parametric model. The modelling framework also includes the full interaction of wave and tides, as well as the combined wind and wave energy resources for the co-located exploitations.

2. Background

2.1 Study area

The study area covers a domain from 105°E to 140°E and from 15°N to 41°N, as shown in Fig. 1.

According to the “Measures for the management of offshore wind power development and construction” produced by the Ministry of Natural Resources of the People’s Republic of China in 2011 [42], the offshore wind farms should be constructed at the places where the water depth is greater than 10 m and the distance is more than 10 km from the shoreline to minimize the influence of constructions to the coastal environment. On the other hand, the construction and maintenance of energy converter devices or the energy transfer devices should be located more conveniently in the shallow water areas. For those reasons, 15 nearshore representative locations within a water depth between 20 m to 40 m along the China coasts are selected in this study to assess the wind and wave energy potential in the nearshore area. Their locations and water depths are shown in Fig. 1 and Table 1. Amongst, P1 to P3 are located in the Bohai Sea, P4 to P6 in the Yellow Sea, P7 to P10 in the East China Sea, and P11 to P15 are located in the South China Sea.

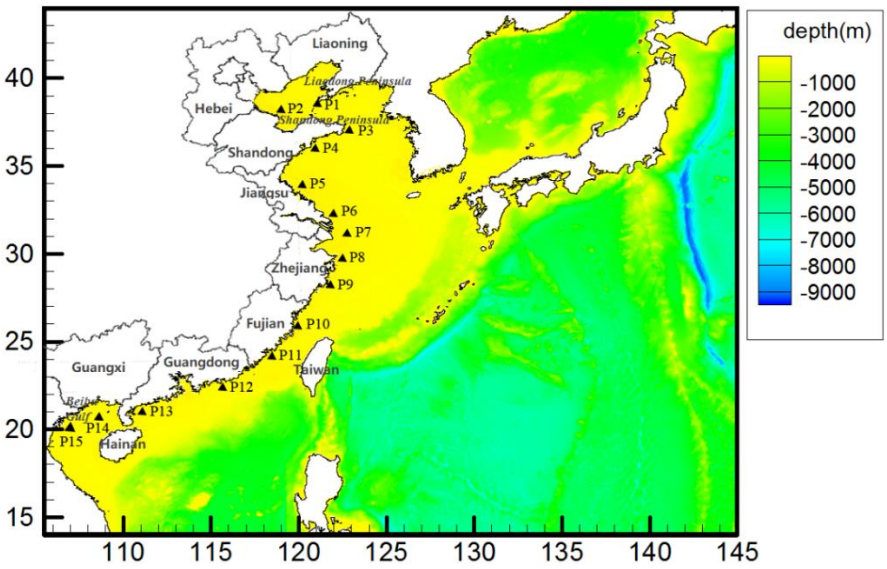

Fig. 1 The study area and the representative locations

Table 1 Location and water depth of the representative coastal locations

	Longitude (°)	Latitude (°)	Depth (m)
P1	121	39	32.5
P2	119	38.4	21
P3	123	37.1	28.5
P4	120.8	36.1	24
P5	120.7	34.7	20

P6	122.2	33	23
P7	122.7	31.1	26
P8	122.6	29.7	33
P9	121.9	28.2	26
P10	119.9	26	21
P11	118.4	24.3	20
P12	115.5	22.6	25
P13	111.2	21.2	21
P14	109	20.5	35
P15	107.5	20	29.5

2.2 Tropical Cyclones

Tropical cyclone (TC) is a rapidly-rotating storm system characterized by a low-pressure centre and strong winds. The TC events often occur with strong winds, can always generate extremely large storm waves. The China seas, which located in the northwest Pacific Ocean, are frequently attacked by TCs. Based on the maximum velocity near the centre (Vmax), the TCs can be classified into 6 categories as listed in Table 1, according to the Chinese standard of tropical cyclone classification (GB/T 19201-2006).

Table 1 Classification of TCs (Chinese Standard - GB/T 19201-2006)

Category	Tropical Depression (TD)	Tropical Storm (TS)	Severe Tropical Storm (STS)	Typhoon (TY)	Severe Typhoon (STY)	Super Typhoon (SuperTY)
Vmax (m/s)	10.8 - 17.1	17.2 – 24.4	24.5 - 32.6	32.7 – 41.4	41.5 – 50.9	>51.0

Over the study area, Fig. 2 shows the number of TCs during the years from 1979 to 2013. On average, 25 TCs occurred annually in the northwest Pacific Ocean. The year with the largest numbers of TC is 1994 with 37 TCs observed, while the year with the least numbers of TC is 1998 with only 12 TCs observed. Besides the frequency of TCs, their intensity also has impacts on the wave distribution in the study area. High intensity TCs with larger Vmax tend to generate larger waves. Particularly, for more extreme events, the number of STY and SuperTY occurred each year as shown in Fig. 2 is high. On average, 5 STYs and 4 SuperTYs were recorded each year, but in 1997 and 2006, 8 SuperTYs

alone were recorded. Clearly, the study area has been constantly affected by TCs, with considerable numbers of STYs and SuperTYs, which makes the inclusion of the TCs impacts in assessing both wind and wave energy more important.

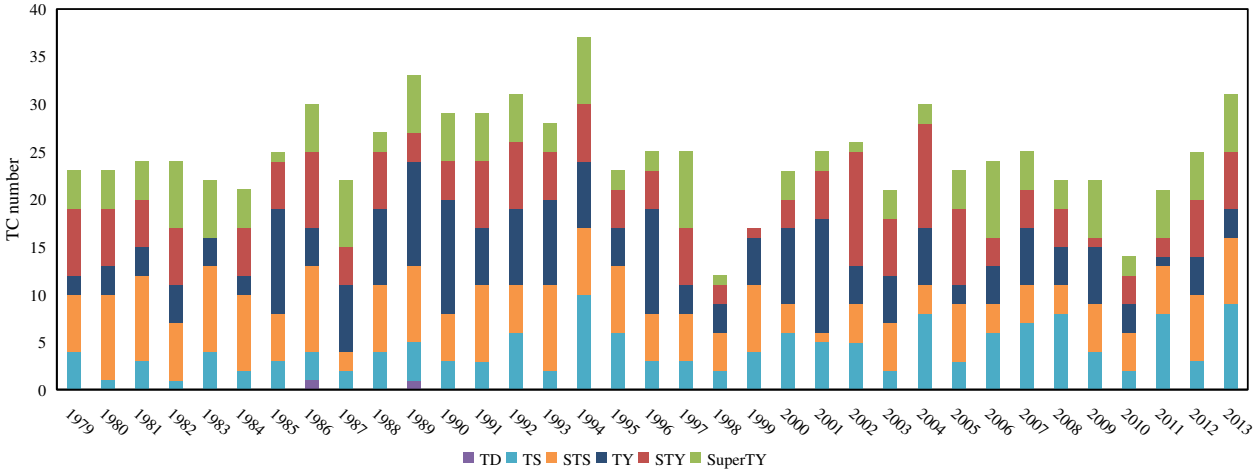

Fig. 2 Annually occurrence of TCs in the northwest Pacific Ocean

As one would expect, the occurrence of the TCs has a strong seasonality in the study area. Fig. 3 shows the monthly distribution of TC numbers between 1979 and 2013. It is clear that numbers of TCs are much higher in the summer and autumn seasons than other seasons. During 1979 to 2013, over 85% of TCs were generated in the period from July to November. September is the month with the largest number of TCs, i.e. 179 TCs.

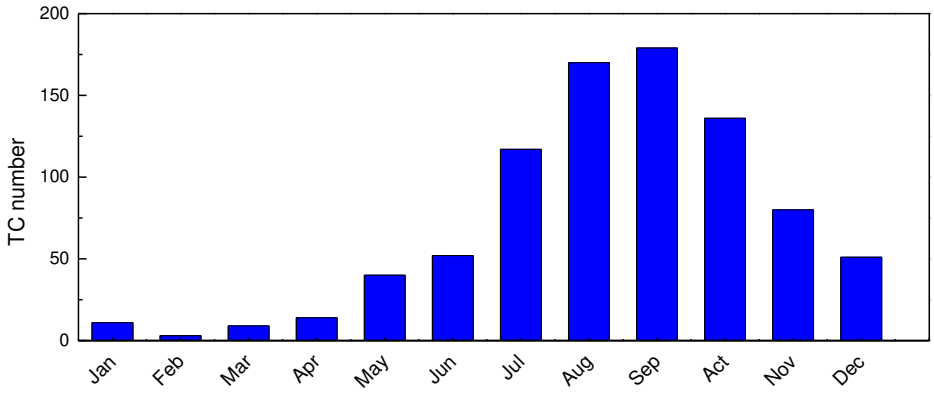

Fig. 3 Monthly distribution of TC numbers between 1979 and 2013

TCs also have a strong spatial variability. Fig. 4 shows the TC tracks over the 35-year period from 1979 to 2013 in the area of the western Pacific Ocean, i.e. the study area. It can be seen that the

southeast part of the China seas is most likely to be affected by TCs with high intensity. The TC tracks shown in Fig. 4, also indicate that the 15 representative locations can be distinctly classified into two categories, i.e. the locations lightly affected by TCs in the north (P1 to P6) and the locations strongly affected by TCs in the south (P7 to P15).

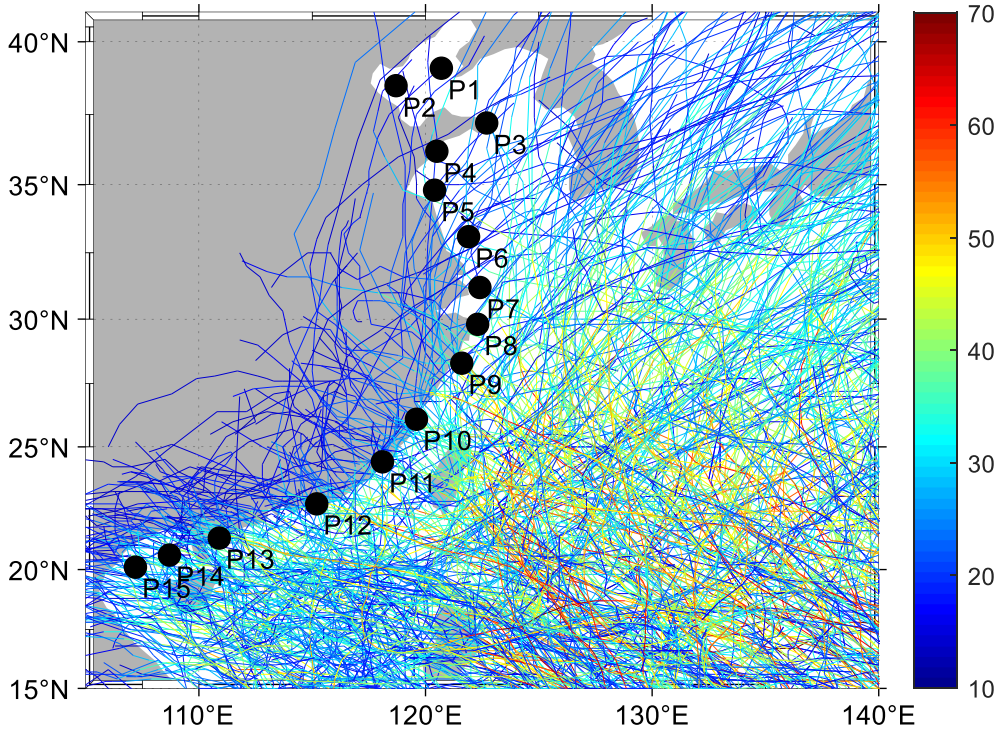

Fig. 4 The TC tracks over 35 years from 1979 to 2013 (color indicates the maximum wind speed at TC centre)

3. Methodology

3.1 Wind and wave data

In this study, the 6-hourly wind data at 10 m above the sea surface from the ECMWF ERA-Interim global atmospheric reanalysis is used as the background wind conditions. The spatial resolution of the ECMWF wind data is approximately 79 km on the reduced Gaussian grid, and is interpolated to 0.125° grid. The existing resolution of reanalysis wind data provided by ECMWF, as suggested by earlier studies [16,43-44], is insufficient to represent the atmospheric forcing of TC events. Therefore, a parametric TC model as introduced by Jelesnianski [45] is used to generate TC wind field near the TC centre for a better representation of the TC's effects. Guided by the measured information along the TC tracks, the parametric TC model modifies the wind and sea surface pressure fields at the TC centres

and the adjacent area. Then the modified wind and sea surface pressure are blended with the ECMWF ERA-Interim wind data, which results in the blended wind and sea surface pressure data being re-constructed as the primary surface forcing for wave modelling and the consequent assessment of wind and wave energy in the study area. The wind data is well validated using the measuremens. The details of the construction and validation of the blended wind field can be found in [46,17].

The wave data used in this study is obtained from the model simulations using a coupled modelling framework of FVCOM circulation model with an unstructured grid, finite-volume surface wave model FVCOM-SWAVE developed by Qi et al. [47], which is driven by the blended wind forcing described previously, with the output at hourly intervals. This model is well validated using the measurement data. The modelling system, and further details of the model setup and validation results can be found in [17].

3.2 Wind and wave energy

The wind energy density (WIED) is greatly dependent on the wind speed and air density. It can be estimated by [20],

$$P_{wind} = 0.5\rho V^3 \tag{1}$$

where ρ is the air density (1.292 kg/m^3) and V is the wind speed at 80 m (the common installation height of WTs) above the sea level. In order to convert the wind speed from that at 10 m above the sea surface of the blended wind data, the logarithmic law is applied [31]:

$$V_{80} = V_{10} \cdot \ln\left(\frac{80}{z_0}\right) / \ln\left(\frac{10}{z_0}\right) \tag{2}$$

where V_{10} is the wind speed at 10 m above the sea level; and z_0=0.2mm is the roughness factor of the calm sea surface.

The potential wave energy density (WAED) in deep water is directly related to the wave height and wave period. It can be estimated empirically with the following expression [48],

$$P_{wave} = 0.49 H_s^2 T_e \quad (3)$$

where H_S is the significant wave height and T_e is the wave energy period defined in terms of moments of the wave spectrum as:

$$T_e = \int_0^\infty f^{-1} S(f)\, df \,/\, \int_0^\infty S(f) df \quad (4)$$

where f is the wave frequency and $S(f)$ is the wave energy spectrum density. The wave period calculated by the FVCOM-SWAVE model is the peak wave period T_p. The relation between T_e and T_p can be expressed as:

$$T_e = \alpha T_p \quad (5)$$

where α depends on the shape of the wave spectrum [20]. In this study, a conservative approximation, $\alpha = 0.9$, is adopted, assuming that the sea state in the study area can be represented by a standard JONSWAP spectrum [49]. The effect of water depth is considered when calculating the wave energy flux at locations with shallow or moderate water depth by incorporating the wave velocity [50].

To evaluate the impacts of TCs on the distribution of wind and wave energy resources, two scenarios are considered and compared in this study: one with TCs being included and the other with TCs being excluded. For the cases with TCs being included, the wind and wave energy densities are assessed directly using the blended wind field and wave field generated by it from the FVCOM-SWAVE model. However, for the cases with TCs being excluded, the wind and wave energy densities around the TC centres (within 3 degrees) during the period of each TC event are masked. The locations of TC centre, the start and end times of each TC event are defined by the measurement data from the "best track dataset" provided by China Meteorological Administration Tropical Cyclone Data Center (http://tcdata.typhoon.gov.cn/) [51].

3.3 Combined wind and wave energy

The simultaneous exploitation of the co-located wind and wave energies could increase the energy yield at lower costs especially when the resources are not temporally correlated [33]. However, wind

and waves may be highly correlated, therefore, it is also important to quantify the correlation between wind and wave resources.

Correlation coefficient (R coefficient) defined by Ferrari et al [33] is applied to describe the correlation between wind and wave energy potential at any location in the study area with the following equation,

$$R_{(wind,wave),i} = \frac{Cov_{(wind,wave),i}}{\sigma_{(wind),i}\sigma_{(wave),i}} \tag{6}$$

where $\sigma_{(wind),i}$ and $\sigma_{(wave),i}$ are the standard deviations of wind and wave energy potential time series at the ith grid point, and $Cov_{(wind,wave),i}$ is the covariance between the two temporal series, defined as,

$$Cov_{(wind,wave),i} = \frac{1}{N-1}\sum_{k=1}^{N}(P_{wind_k} - \overline{P_{wind}})(P_{wave_k} - \overline{P_{wave}}) \tag{7}$$

A higher value of R indicates a higher correlation between wind and wave energy potential.

To estimate the exploitable wave energy, the power matrix of the PPC WEC systems as shown in Fig. 5(a) with the rated capacity 3.6 MW is used as an example [31], while for exploitable wind energy, the power curve of wind turbine SWT-3.6-120 as shown in Fig. 5(b) for the same rated capacity 3.6 MW as the PPC devices is used.

(a)

Significant wave height (m) \ Energy period (s)	4	5	6	7	8	9	10	11	12	13	14	15	16
1	180	166	153	171	125	87	72	65	85	85	37	29	16
1.5	223	195	157	148	261	192	223	139	155	155	74	67	46
2	0	0	214	227	396	335	237	235	182	138	115	104	70
2.5	0	0	0	440	598	514	376	342	204	169	142	128	95
3	0	0	0	681	801	735	594	486	199	175	151	134	121
3.5	0	0	0	904	1035	949	788	617	239	209	183	164	146
4	0	0	0	1131	1269	1163	982	743	285	248	216	195	175
4.5	0	0	0	1358	1488	1374	1187	869	330	287	250	225	201
5	0	0	0	1585	1712	1585	1392	988	380	334	285	263	226
5.5	0	0	0	1812	1937	1798	2138	1107	429	381	323	301	261
6	0	0	0	2040	2162	2010	2884	1234	439	416	361	336	295
6.5	0	0	0	2267	2386	2221	3143	1360	449	450	406	372	329
7	0	0	0	2494	2611	2433	3619	1483	506	464	451	408	363

(b)

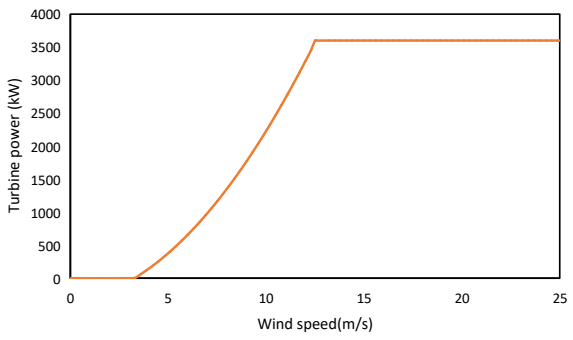

Fig. 5 *Power output for (a) WEC and (b) WT (adopted from [31])*

4. Wind Energy Density

4.1 Mean wind energy density

WIED is calculated using Eq. (1) over the 35-year period in the study area for the cases of including and excluding TCs. Fig. 6 shows the distribution of mean WIED over the 35-year period. The results show that the WIEDs in the China seas are over 800 W/m^2 in general, but it can reach 1400 W/m^2 in the southeast part of China seas, where the mean WIED for the case including TCs is obviously seen larger than that excluding TCs in an order of 200 W/m^2 approximately. This indicates that the TC events can considerably affect the distribution of wind energy especially in the southeast area of China seas, where it becomes necessary to take full consideration of the frequently occurred TC events in this area when assessing the wind energy.

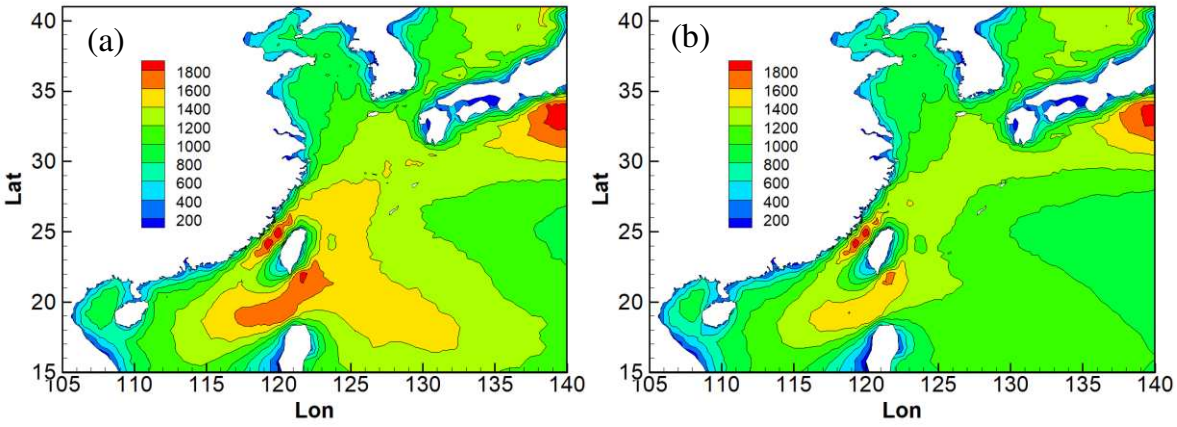

Fig. 6 Multi-year (1979 – 2013) mean wind energy density (W/m^2) for the cases of (a) including TCs and (b) excluding TCs

Considering the commonly used type of WTs in China [52], the cut-in speed (the lowest threshold for electrical generation) and cut-out speed (the highest threshold for electrical generation) are generally 3 and 25 m/s while the survival speed are generally between 50 to 60 m/s. Fig. 7(a) shows the exploitable 35-year mean WIED in the study region with wind speed between 3 to 25 m/s. Fig. 7(b) shows the proportion of available time of electrical generation (availability rate) in 35 years. In general, the availability rate of wind power could be over 90% in the offshore China if only consider the cut-in and cut-out wind speed. Comparing Fig. 7(a) with Fig. 6(b) shows that exploitable wind energy in the

study area is close to the distribution as shown in Fig. 6(b) for the case excluding TC, as the events of extreme TCs may contribute little to the overall power generation due to the high wind speed exceeding the thresholds of the devices. Therefore, the further analysis in this study uses the exploitable energy rather than the potential energy.

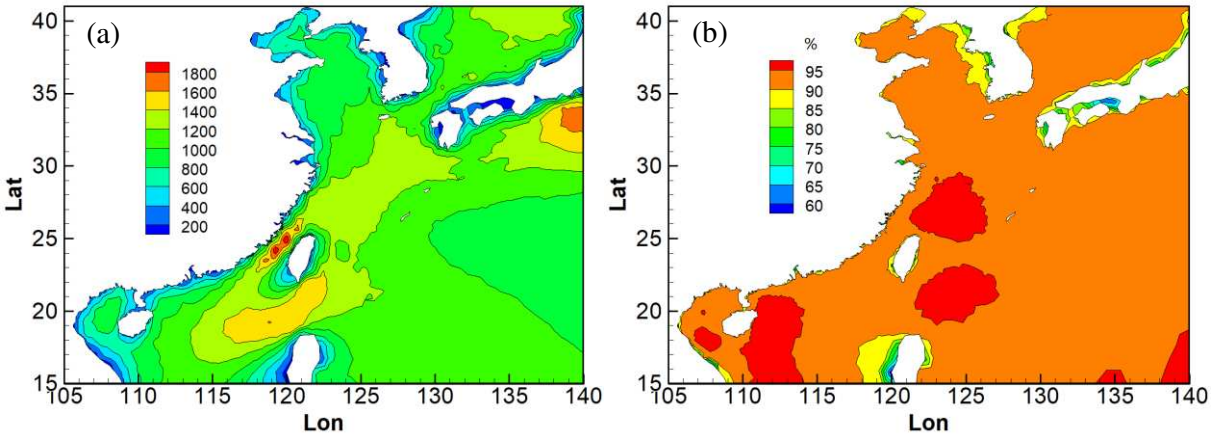

Fig. 7 The distribution of (a) exploitable multi-year mean wind energy density (W/m^2) and (b) proportion of available time for power generation

4.2 Seasonality of wind energy

As the climate in the China's coastal waters exhibits a distinct seasonality, the distribution of 35-year mean WIED in four seasons is also calculated (using the exploitable data). Fig. 8 shows the seasonal distribution of mean WIED in the study domain. As expected, the mean WIED in the winter and autumn seasons is larger than those in the spring and summer seasons. In the spring and summer seasons, the mean WIED is between 400 to 1000 W/m^2 over the sea, while in autumn, it is between 800 to 1800 W/m^2. In winter, the mean WIED is greater than 1400 W/m^2 in most of the sea areas, especially in the southeast, indicating abundant wind energy exploitable in winter in the region.

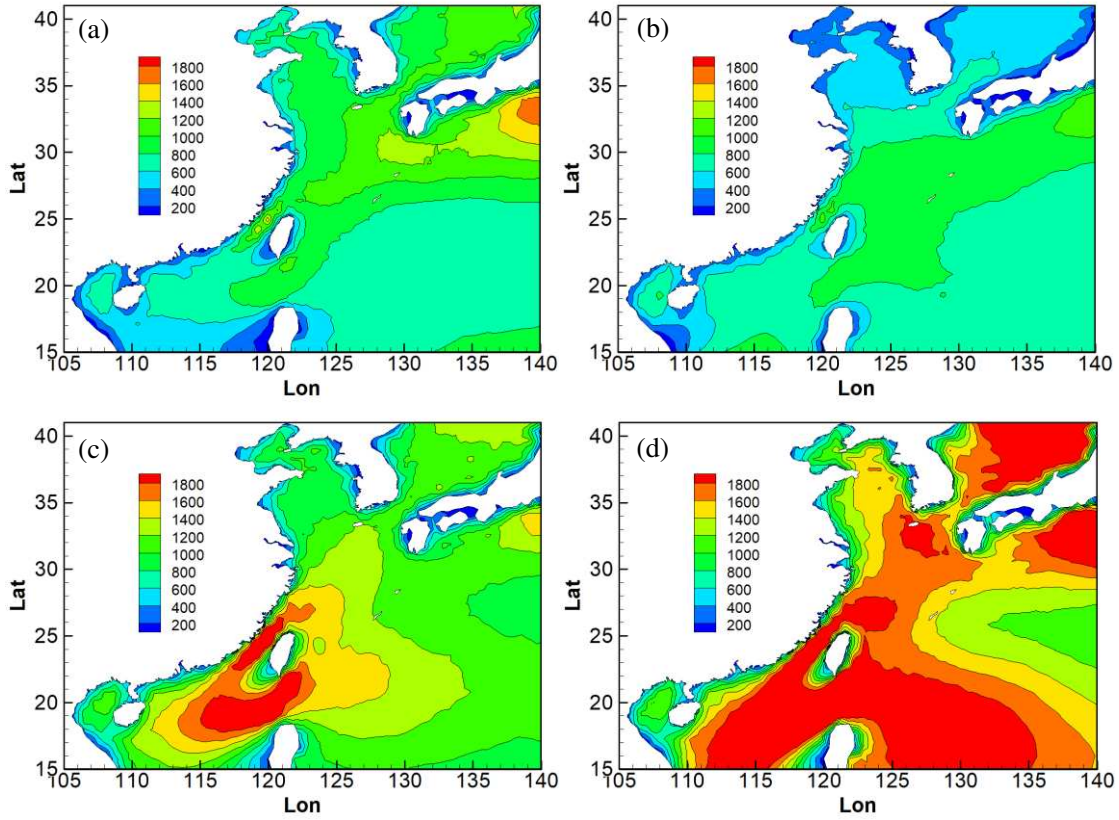

Fig. 8 The seasonal distributions of exploitable multi-year mean wind energy density (W/m^2) in (a) spring; (b) summer; (c) autumn; and (d) winter

4.3 Effects of TCs on wind energy

To further illustrate the effects of TCs on the wind power potential, two representative years, i.e. 2010 and 2013, are selected, where the former represents the year lightly influenced by TCs and the latter represents the year strongly influenced by TCs, to illustrate the effects of TCs on the seasonal wind energy density distributions. The total numbers of TCs and SuperTCs in 2010 are 14 and 2 respectively, in comparison with 31 and 6 respectively in 2013, indicating that both frequency and intensity of TCs in 2013 are larger than 2010. All those TCs are well described in the analyzed data. Fig. 9 shows the seasonal distribution of the annually average wind energy density in 2010 and 2013. It can be seen that except for spring, the WIED in 2013 are generally higher than that in 2010. Particularly, in autumn, the WIED in 2013 is significantly higher than that in 2010, which the difference could be over 400 W/m^2, due to the significant contribution of the TCs in the potential wind energy yielding. The frequency and intensity of TCs have great impacts on the distribution of wind resources in China seas.

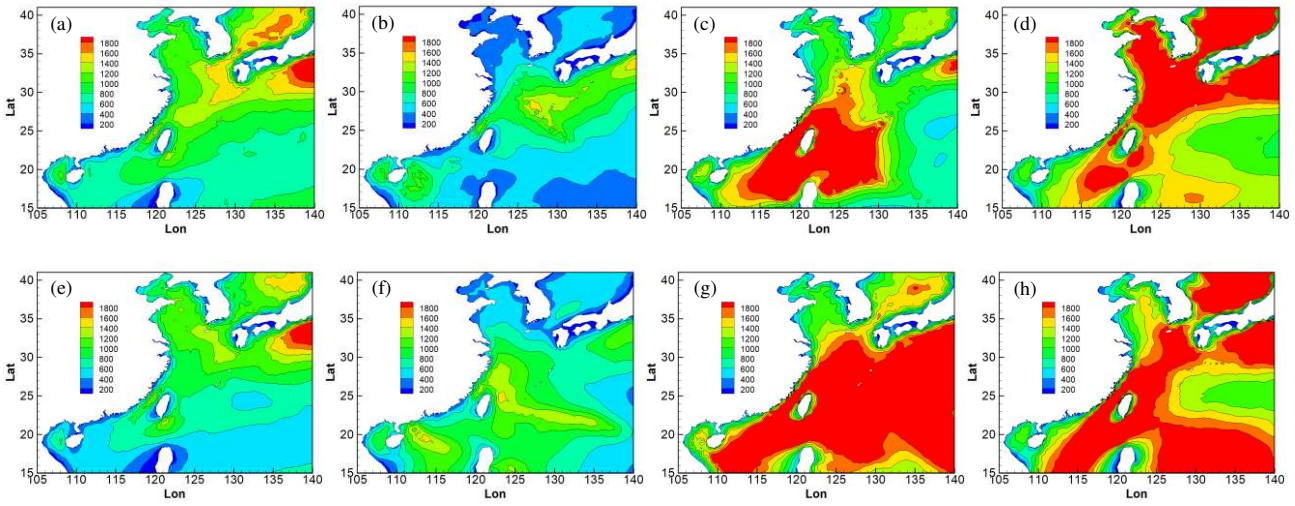

Fig. 9 Seasonal distributions of the multi-year mean wind energy density (W/m^2) in spring, summer, autumn and winter (from left to right; top panels for 2010 and bottom panels for 2013; TCs included)

4.4 Safety of energy exploitation

To evaluate the risks of operation of WTs under extreme winds, the durations (in hours) of the wind speed in the study area exceeding the thresholds that correspond to 3 severe TC categories: TY (32.7 m/s), STY (41.5 m/s) and SuperTY (51.0 m/s), are calculated. The wind speed of 51.0 m/s is also referred to the practical survival speed of WTs. Fig. 10 shows the hours over 35 years when the wind speeds excess the thresholds described above. It is clear that in the entire coastal area, especially in the East China Sea, the number of hours for wind speed exceeding 51 m/s is extremely low, indicating that it is mostly safe for TWs to be deployed and operated in area. Along the southeast coast of China, the number of hours exceeding 41.5 m/s is less than 60, which also indicates a relatively safe condition for the deployment of WTs. For the entire coastal area, the number of hours over 35 years exceeding 32.7 m/s is generally under 120, which again indicates a relatively good condition of wind resources exploitation.

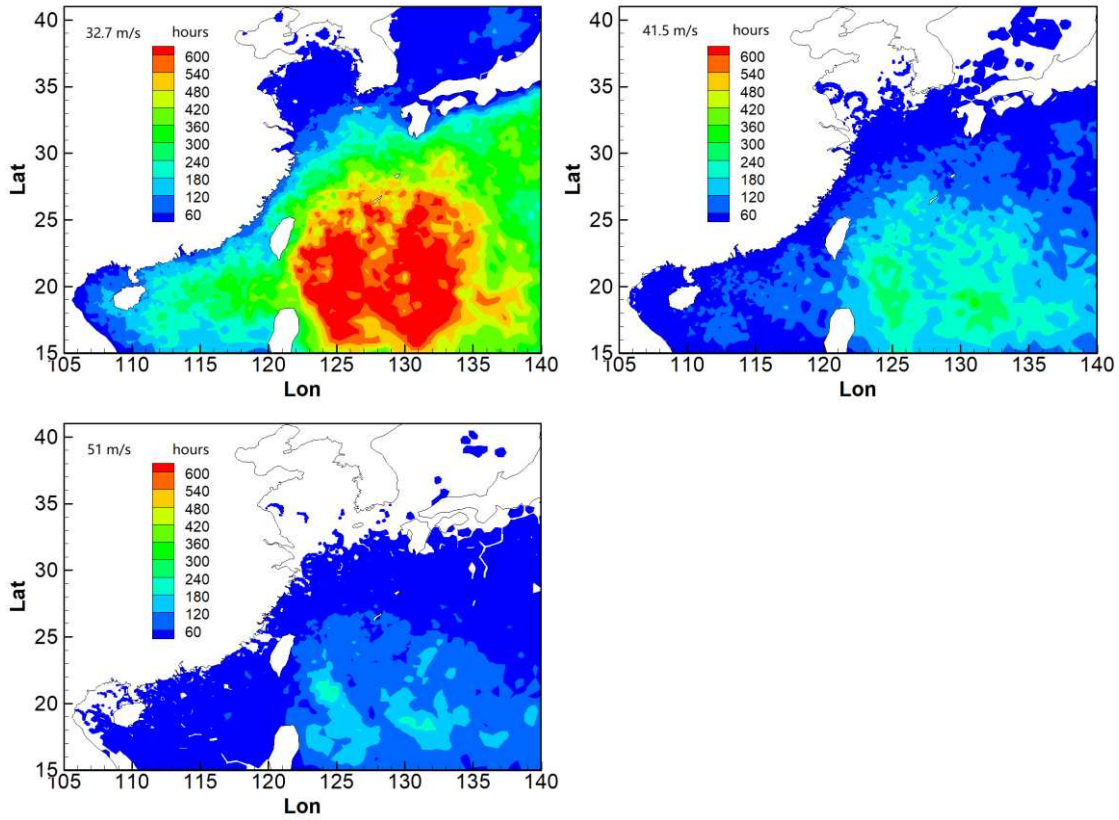

Fig. 10 The duration (in hours) when wind speed exceeding 32.7 m/s, 41.5 m/s, and 51m/s over 35 years from 1979 to 2013

5. Wave Energy Density

5.1 Mean wave energy density

The potential WAED is calculated using Eq. (3) from the wave characteristics generated from the coupled FVCOM and FVCOM-SWAVE model over the 35-year period with blended surface forcing [17]. Fig. 11 shows the multi-year mean wave energy density over 35 years for the cases including and excluding TCs. In general, the WAED when TC effects are included is greater than that when TC effects are excluded, which means that TCs have a noticeable influence on the distribution of wave energy potential. It can also be seen that the mean WAED decreases from deep water towards the coastal area. The maximum WAED appears in the southeast area and is over 18 kW/m for the case including TC effects, which is approximately 2 kW/m larger than that when TC effects are excluded. This highlights the necessity for the TC events to be considered when assessing the wave energy resources for a practical evaluation and also for the safety of WECs.

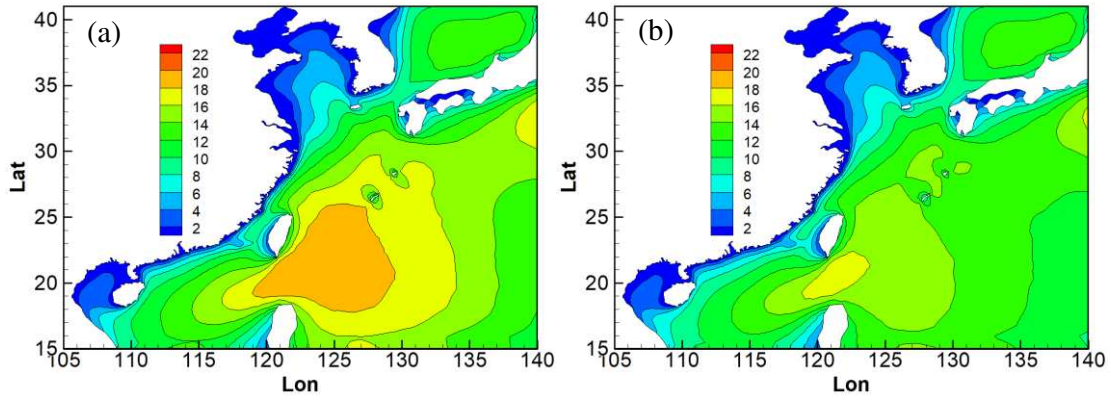

Fig. 11 Multi-year mean wave energy density (kW/m) in the China seas for cases (a) including TCs; and (b) excluding TCs

In investigating the power matrix of several different types of WECs [31], the wave heights between 0.5 to 7 m and the energy period between 4 s to 16 s are considered to calculate the exploitable wave energy. Fig. 12(a) shows the distribution of the exploitable WAED and the general pattern is similar to that shown in Fig. 11(b) for the case excluding TCs. Fig. 12(b) shows the proportion of available time for power generation (utilization rate) relating to wave energy in 35 years. The utilization rate of wave energy is lower than wind energy along the China coast, especially in the East China Sea.

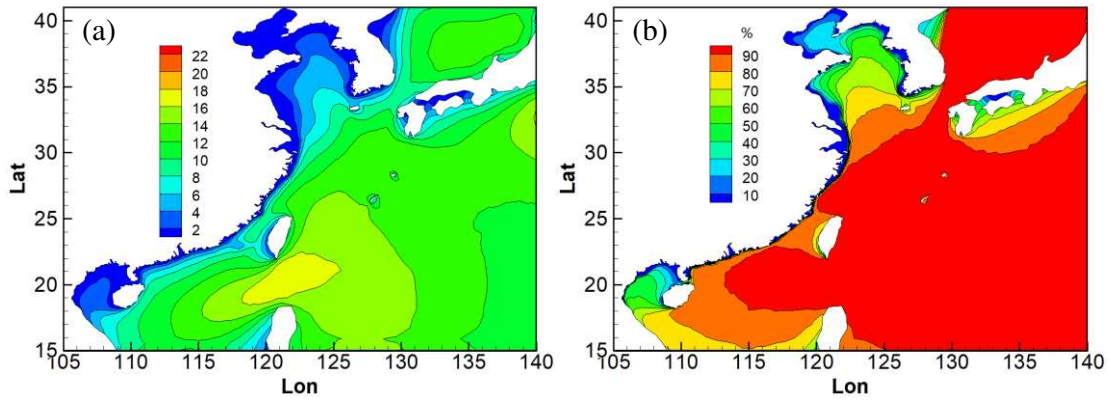

Fig. 12 The distribution of (a) exploitable multi-year mean wave energy density (kW/m); and (b) proportion of available time for power generation

5.2 Seasonality of wave energy

The seasonal distributions of mean WAEDs are also analyzed, as shown in Fig. 13. The mean WAEDs

in the Bohai Sea are generally under 2 kW/m in spring and summer seasons while under 4 kW/m in autumn and winter seasons. In the East China Sea, the mean WAEDs increase from the north to the south. The southeast part of China seas appears to have the largest energy potential, which can reach 22 kW/m in the autumn and winter seasons. Different from the distribution of mean wind power which has the largest value in winter, the mean WAED in autumn appears to be a little larger than that in winter especially in the East Sea and the east area of Taiwan island. This is because the WAED is not only related to the wave height (closely related to wind speed) but also the wave period. In summary, the potential wave energy resources in the autumn and winter seasons are more plentiful than the other two seasons and the area in the south of the study domain is found to possess the largest amount of wave energy potentials.

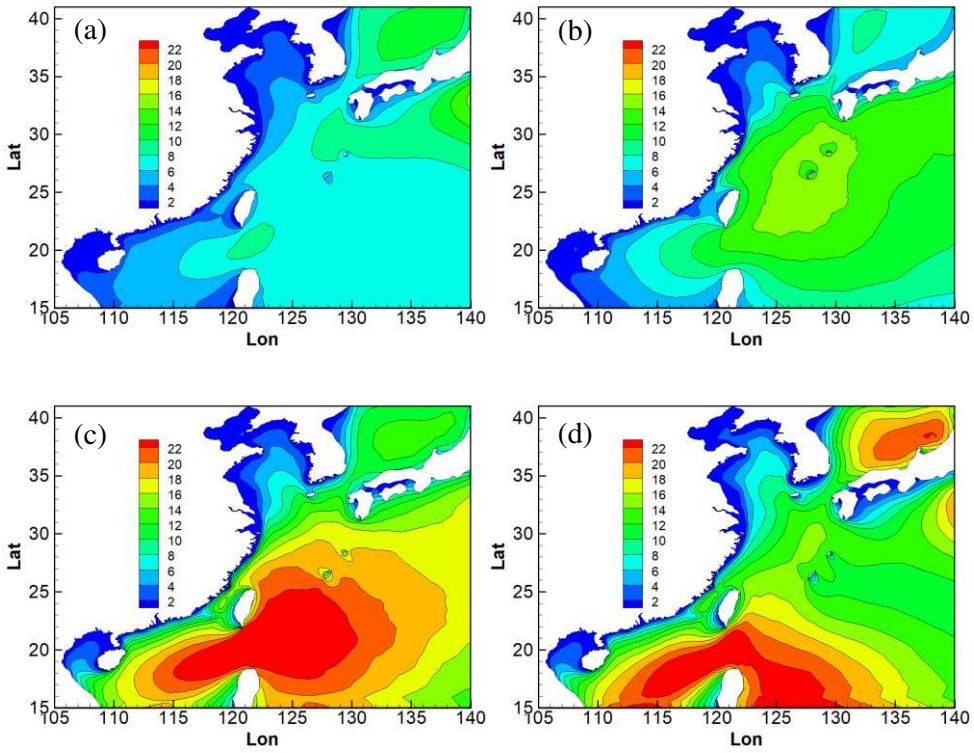

Fig. 13 The seasonal distributions of multi-year mean wave energy density (kW/m) in (a) spring; (b) summer; (c) autumn; and (d) winter

5.3 Effects of TCs on wave energy density

Similarly, Fig. 14 shows the distribution of mean wave energy density in four seasons in 2010 and 2013, which represent the lower and higher years for TCs. It can be seen that the wave power in autumn

season is significantly larger than other seasons. Comparing the years 2010 and 2013, the magnitude of wave power in spring, summer and winter seasons are similar. In autumn, the wave power in 2013 is larger than that in 2010 which is due to the larger frequency and intensity of TCs in 2013. For the autumn season in year 2013, the wave power in the south part of the East China Sea, the north part of the South China Sea and the east adjacent sea areas are larger than 22 kW/m. For TC affected areas, the frequency and intensity of TCs could greatly change the local distribution of wave power.

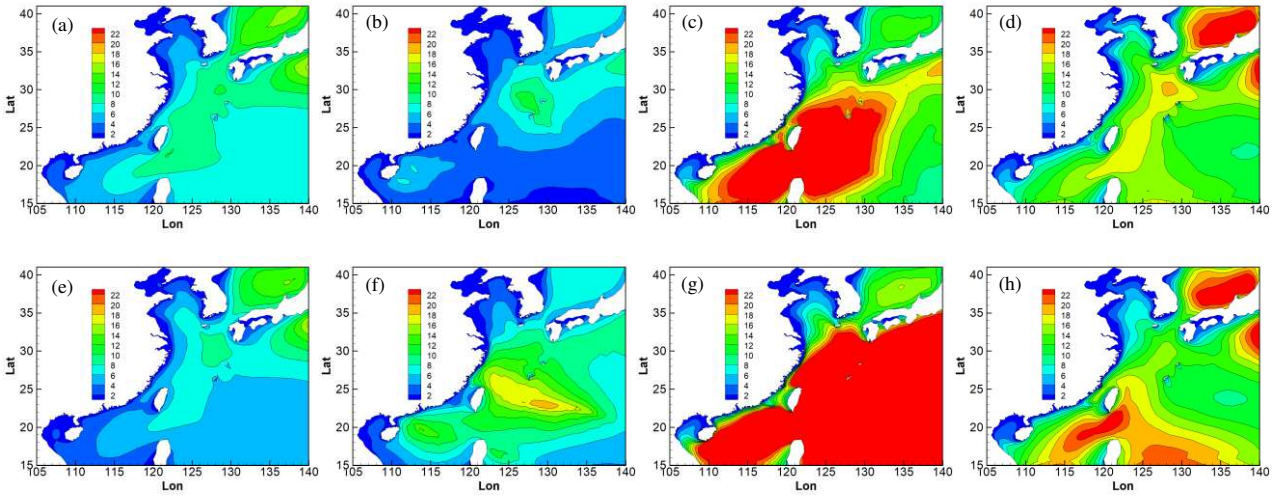

Fig. 14 Seasonal distributions of mean wave energy density (kW/m) in spring, summer, autumn and winter (from left to right; top panels for 2010 and bottom panels for 2013; TCs included)

6. Combined wind and wave energy generation

The multi-year mean total power generated from wind and waves is calculated using the method described in Section 3.3. Fig. 15 (a) & (b) show the mean annual total power generated from wind and wave with the exemplary devices previously described. Similar to their energy density distributions, both types of marine energy are richer in the deep ocean than those in the coastal waters, but less exploitable technologically and economically. Focusing on the nearshore waters, the exploitable wind power can be up to 3GW annually along the coastline of China, whilst the annual wave power is relatively lower in the range of 300 MW in the central and south parts of the coastline. Along the coasts of the Bohai Sea and the Yellow Sea, the annual wave power generation is the lowest, below 100 MW, where exploitation may by unavailable.

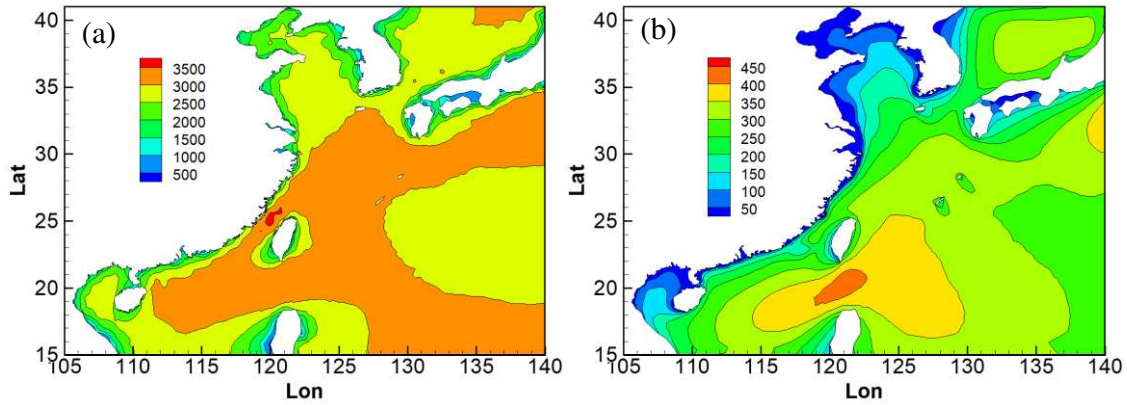

Fig. 15 Distribution of multi-year mean total power (MW) generated from: (a) wind; and (b) wave

The proportion of wind energy in the combined energy is shown in Fig. 16. The wind energy has a greater share in the total energy in the deep water area, which indicates the rich potential wind energy in China seas to be exploited. This is also evidenced by the growing construction of the wind farms along many China coasts [53], also supported by the fact that the technique of WTs becomes more mature than the WECs. For the WTs and WECs with the same capacity rate, the energy conversion efficiency of WTs is currently greatly larger than that of WECs, but with the further development of WEC technology and efficiency, the integration of co-located wind-wave convert devices would help the large-scale exploitation in China in the near future.

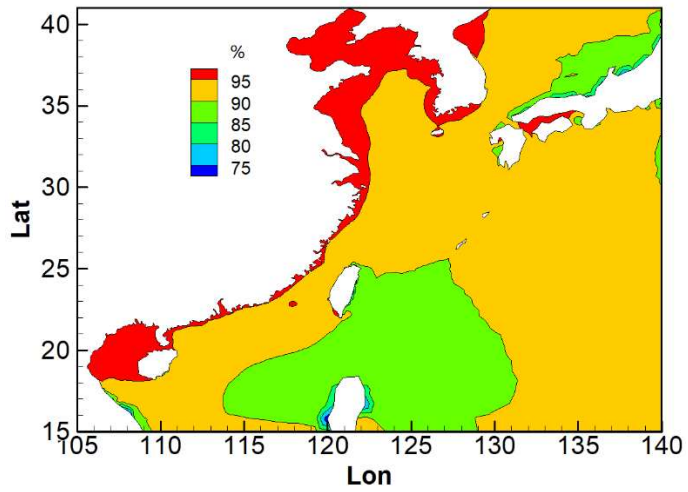

Fig. 16 Proportion of wind energy in the combined energy

Combining the mean annual power generated from winds and waves (Fig. 15) gives the total annual

power generation from both types, as shown in Fig. 17(a). It is clear that the distribution is dominated by the wind energy as expected. However, the correlation of the wind and wave energy generation is also a key factor in determining the optimal co-location of the exploitation. In general, when the wind and wave resources are not temporally correlated, they could contribute to a better use of the natural resources in view of the construction of co-located wind-wave farm, as they will generate power during different time periods [33]. According to the method introduced in Section 3.3, Fig. 17(b) shows the distribution of the correlation coefficient R. In nearshore areas, coefficient R is generally under 0.6 except in the Bohai Sea and the Yellow Sea. The areas that have relatively low correlations between local wind and wave energy resources are the coasts of Zhejiang and Guangdong Provinces. By comparing Fig. 17(a) and Fig. 17(b), it can be seen that the Taiwan Strait is a typical area (red box) with high energy potential and high correlations. The coastal area of Zhejiang Province, the southern coastline of Guangdong Province and the southern coastline of Shandong peninsula are the typical area (blue box) for medium energy potential and low correlations which could be the potential site for the co-located wind-wave farm. The Bohai Sea and the Yellow Sea (black box, except for the southern coastline of Shandong Peninsula) have relatively low energy potential and high correlations which may be unsuitable for co-located wind-wave farms.

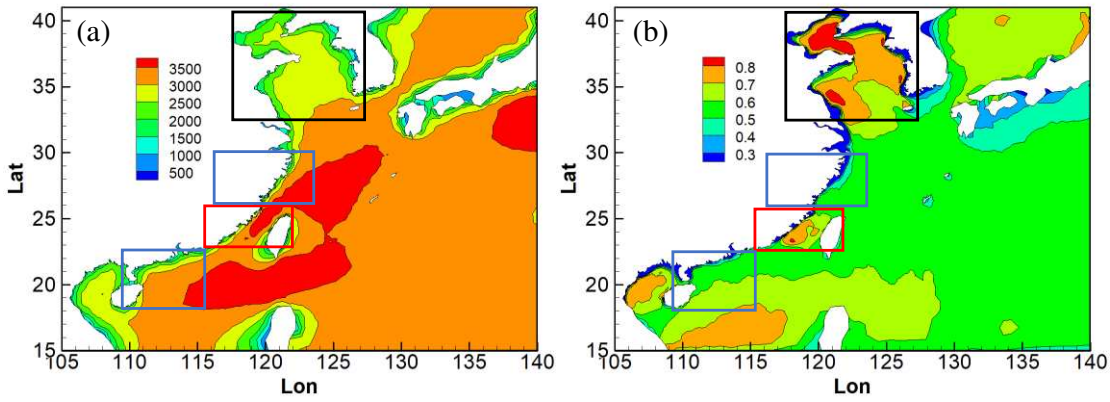

Fig. 17 Distributions of (a) combined wind and wave energy; and (b) correlation coefficient R

7. Potential site selection

As the wind and wave energy resources in the nearshore area are easier to collect and transfer, the distributions of wind and wave energy potential in coastal waters of China at 15 representative

locations indicated in Fig. 1 and Table 1 are assessed.

7.1 Wind and wave energy at representative locations

Fig. 18 shows the 35-year mean WIEDs and WAEDs at 15 selected locations. Among all the representative locations, P9 which locates on the east coast of China appears to have the largest WIED and WAED, i.e. 1168 W/m^2 and 7.56 kW/m. For other locations on the east coast, i.e. P6 to P11, the WIEDs are generally over 800 W/m^2 and the WAEDs are generally over 3 kW/m. P1 and P3 that locate in the Bohai Sea also have relatively large WIED which means the wind resources in Bohai Sea are plenty. Along the mainland coast of the South China Sea, the WIED and WAED at P15 is relatively high while that at P12 to P14 are relatively low. In summary, in the coastal waters of China, the areas around the head of Liaodong peninsula and Shandong peninsula, the east coast of Zhejiang province, the east coast of Fujian province and the west coast of Beibu Gulf are appearing to have plenty of wind energy resources. P9 at the north of Zhejiang coast and P11 at the south of the Fujian coast tend to be the most resourceful in terms of wave energy among all the representative locations. On the other hand, for P5 and P6 at the Jiangsu coast, the wave energy are the poorest. Although the wave energy resources in the north are not as plenty as the south area, P3 at the head of Shandong Peninsula still has a relatively good performance.

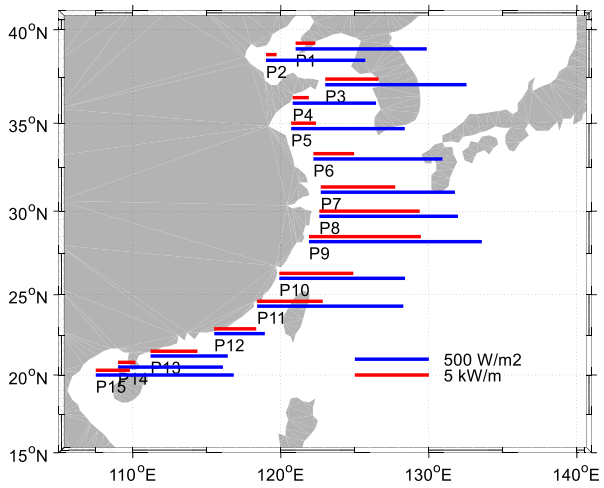

Fig. 18 Multi-year mean WIED (blue) and WAED (red) at the representative locations

7.2 Directional distributions of wind and wave energy

Although WIED and WAEDs are the key elements for deploying the WTs and WECs, the consistent wind and wave direction is also important at the site. Fig. 19 shows the WIED roses at 15 representative locations (the directions in bearings). At P1, P2, P5 and P6, the wind directions are diverse, which may not be ideal places for WTs. At P3 and P4, southernly and northernly winds are dominant. At P8 and P9, NNE is the dominant wind direction and winds from N and NNE directions tend to have higher wind energy potential than other directions. At P10 to P15, NE is the dominant wind direction. Among them, especially at P10 and P11, the NE direction WIED takes over 30% of the total energy. Considering the values of WIED, areas at P8 to P11 can have the largest wind energy potential among all the representative locations; and in contrast, areas at P12 and P13 have the least value of WIED.

The directional characteristics of the WAED is also studied to guide the location selection for deploying the WECs. The WAED roses are shown in Fig. 20 from the modeled wave data over 35 years. It can be seen that N is the dominant wave direction of P1, S is the dominant wave direction of P3 and SSW is the dominant wave direction of P14. Except for P1, P3 and P14 locations, the dominant wave directions of other locations are between NNE to SSE. Due to the orientation of the coastline, the easterly waves are dominant. Particularly, at P10 and P11, the wave energy from ENE direction takes over 40% of the total wave energy. Combining Fig. 18 and Fig. 20, the locations at P3, P9 to P12, where wave directions are relatively consistent and WAEDs are of high values, can be the suitable places for the deployments.

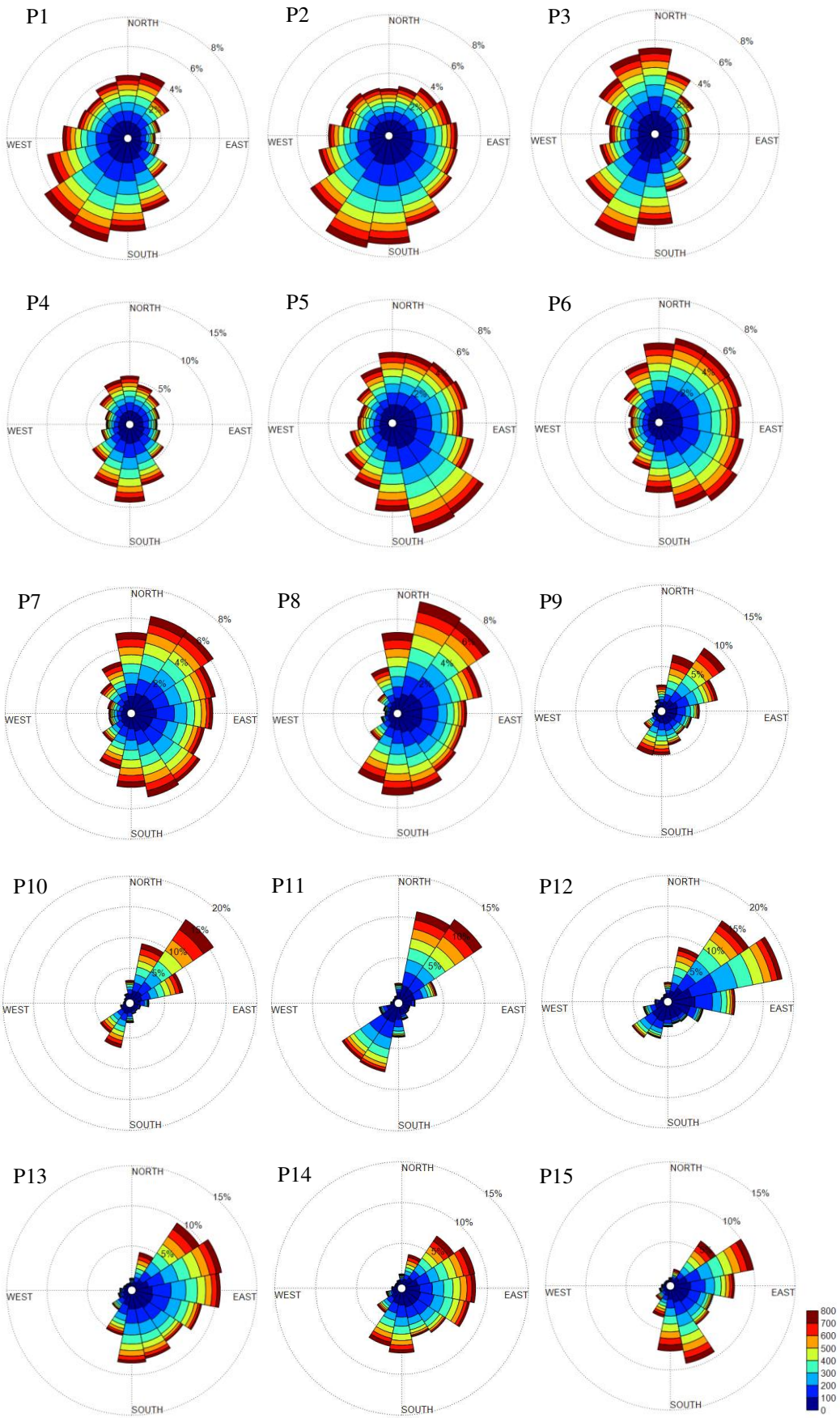

Fig. 19 Wind energy density (W/m^2) roses at 15 representative locations

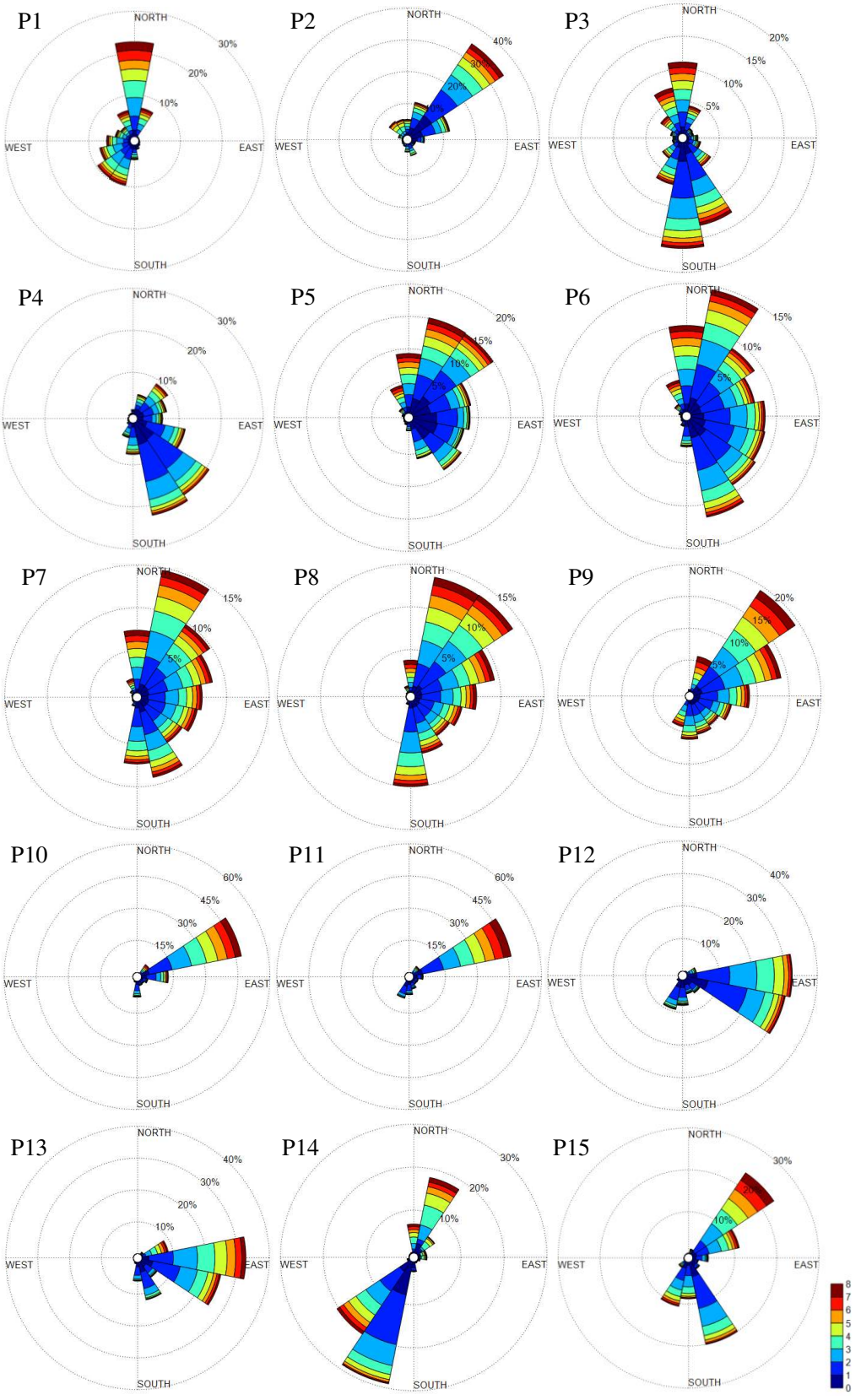

Fig. 20 Wave energy density (kW/m) roses at 15 representative locations

7.3 Bivariate distributions for wave energy

Another important factor for location selection for WECs is the bivariate distributions for wave energy between wave height and energy wave period, which are highly device dependent. The bivariate distributions for the mean wave energy over 35 years at 15 representative locations are shown in Fig. 21. The numbers in Fig. 21 indicate the annually average duration (in hours) with the given significant wave height and period, whilst the colors indicate their contribution to the total annual energy generation (in percentage). The results confirm the abundance of the wave energy resources at P3, and P9 to P12, where wave directions are mostly constrained narrowly, see Fig. 20. In general, the sea states with the significant wave heights between 1.5 and 2.5 m and energy periods between 6 and 7 s contribute most to the wave energy. To deploy WECs at these locations, appropriate power matrix of the WECs should be considered in designs based on the wave conditions mentioned above. However, at P9 and P10, it can be seen a wider spread of the sea state for wave energy generation. Thus, the design of WECs at these locations may be more complex than that at other locations, such as P3, P11 and P12, where the sea states for wave energy generation are rather constrained. It is worthy mentioning that the sea state with the longest duration may not be the same one that contributes the most energy because of its low value of wave height and period.

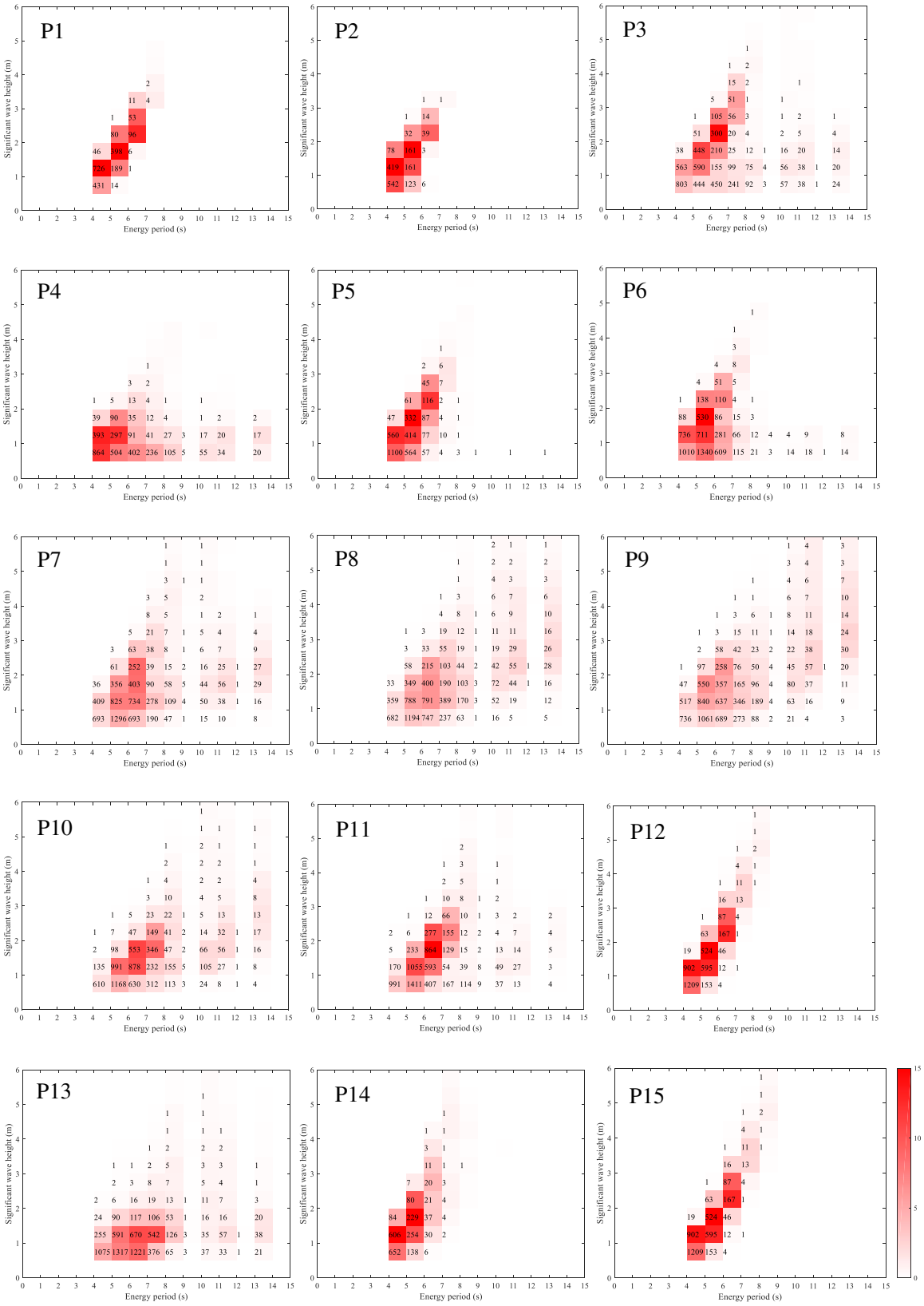

Fig. 21 Bivariate distributions of wave power over the significant wave height and energy period at 15 representative locations (averaged value for 35 years where color represents the contribution of the sea state to

the total energy as a percentage; and number indicates the duration of the sea state in hours)

7.4 Selection of potential sites

Following the evaluation of the distribution of wind and wave energy considering TCs in China seas, the potential sites for the WTs and WECs arrangement are investigated.

Fig. 22 shows the annual total energy power of winds and waves at 15 representative locations and the proportion of available time. The result indicates that at P3 and P4 (along the southern coastline of Shandong Peninsula in the Yellow Sea), and P9 to P11 (along the southeast coast of Zhejiang and Fujian Province) there are high wind energy resources. The proportion of available time of wind resources along the China coast are generally high. Thus, to select the potential site for WT deployment, the southern coastline of Shandong Peninsula in the Yellow Sea, and the southeast coast of Zhejiang and Fujian Province could be good choice. Considering the safety and survivability of WTs, as introduced in section 4.4, the places mentioned above are safe to deploy the wind farm.

Combining the evaluation of mean WAED and scatter diagrams of wave energy along China's mainland coast, the coastal area near Shandong Peninsula, corresponding to representative location of P3, and the coastal areas of Fujian and Guangdong Provinces, corresponding to representative locations at P11 and P12, are found to be the most suitable places for the deployment of WECs. The proportion of available time at these places are over 60%. As P11 and P12 locations are greatly influenced by TCs, by taking the stability of wave energy and survivability of WEC into consideration, the area locates in the head of the Shandong Peninsula can be regarded as a good choice.

Incorporating the effects of TCs, the survivability of energy converter devices are emphatically discussed in this study. It is worth to mention that, on the other hand, with the continuous improvement of TC resistance technology and reliability for WECs, the coastal areas of Zhejiang, Fujian and Guangdong Provinces should also be good choices for the deployment of wave power plant. For the areas of the southern Shandong Peninsula, the southeast coast of Zhejiang Province and the south coast

of Guangdong Province, as they are rich in both wind and wave energy resources, they could be the potential sites for co-located wind-wave farms.

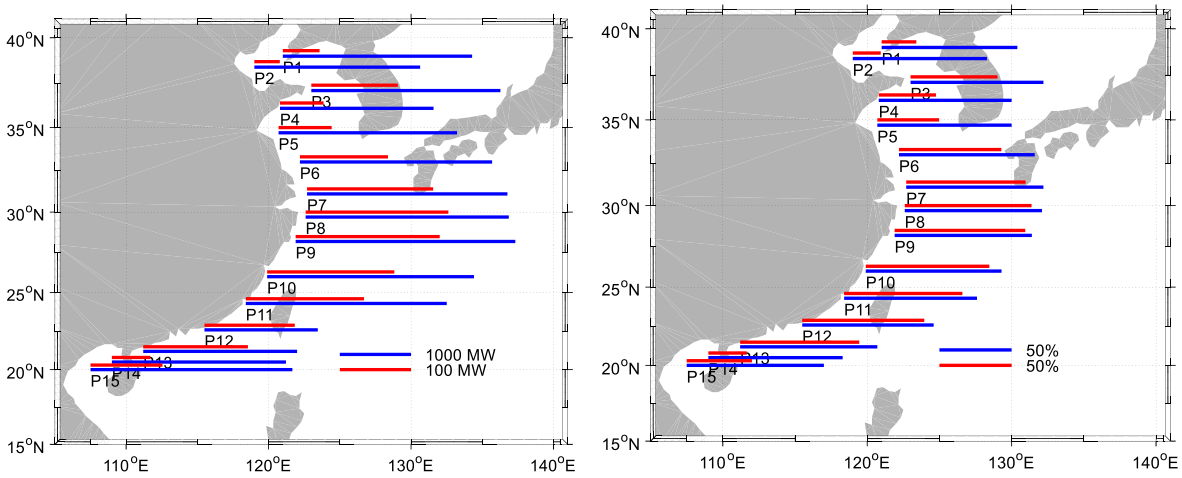

Fig. 22 (a) Annual total power output of wind and wave energy; and (b) proportion of available time for power generation at 15 representative locations

8. Conclusions

The potential wind and wave energy resources in China seas, especially in the coastal waters, are assessed in this paper, with the blended ECMWF ERA-Interim reanalysis wind data from 1979 to 2013 with TCs simulated by a parametric TC model. The results of the multi-year mean, seasonal and directional WIED show that the mean WIED have larger values in the winter and autumn seasons and in the south sea area. The multi-year mean, seasonal and directional WAED, based on the wave characteristics generated from the coupled FVCOM and FVCOM-SWAVE model driven by the blended wind data for the same 35-year period, show that the mean WAED in deep water areas are generally larger than that in nearshore areas, and the WAED in the south are generally larger than that in the north. The effects of tropical cyclones on the distribution of exploitable wind and wave energy are evaluated. The WIED and WAED that including TCs are generally 200 W/m^2 and 2 kW/m larger than that excluding TCs. The TC events could affect the distribution of wind and wave energy especially in the southeast area of China seas.

Combined potential wind and wave energy in the study area is also assessed. Within the total potential

energy from wind and wave energy, the wind energy generally takes over 80% of the total energy. Analysis of the correlation coefficients between wind and wave energy indicates that the coastal area of Zhejiang Province, the southern coastline of Guangdong Province and the southern coastline of Shandong Peninsula are the areas of medium energy potential and low correlations, and can be identified as the potential site for the co-located wind-wave farm.

This study also specially examines the potential wind and wave energy at 15 nearshore locations along the China's coastline. The results indicate that the areas located at the head of Shandong Peninsula in the Yellow Sea, and the areas along the coasts of Zhejiang and Fujian Provinces have high potential for wind energy resources development. For wave energy resources, the southern coastal area of Shandong Peninsula in the Yellow Sea, and the coastal areas of Fujian and Guangdong Provinces are found to be the most suitable places for the deployment of WECs. The results also show that sea states with significant wave heights between 1.5 and 2.5 m and energy periods between 6 and 7 s contribute most to the wave energy generation as indicated at those sites.

The results presented in this paper provide useful guidance for the effective and sustainable development of marine renewable energy in the coastal waters of China.

Acknowledgements

The work was partly supported by the National Natural Science Foundation of China (grant numbers 51909013, 52001031), the Research Foundation of Education Bureau of Hunan Province, China (No. 21B0300, 20B021) and the Open Research Foundation of the Key Laboratory of Water-Sediment Sciences and Water Disaster Prevention of Hunan Province (No. 2021SS05).

References

[1] Saket A, Etemad-Shahidi A. Wave energy potential along the northern coasts of the Gulf of Oman. Iran. Renew Energy 2012;40:90-97. https://doi.org/10.1016/j.renene.2011.09.024

[2] Sahu BK. Wind energy developments and policies in china: a short review, Renew Sustain

Energy Rev 2018;81:1393-1405. https://doi.org/10.1016/j.rser.2017.05.183

[3] Kun W, Yong S. The ocean resources and reserves evaluation in China, 1st national symposium on ocean energy. Hangzhou. China 2008

[4] Boden TA, Marland G, Andres RJ. Global, regional, and national fossil-fuel CO2 emissions. Oak Ridge, Tenn, USA: Carbon Dioxide Information Analysis Center, Oak Ridge National Laboratory. US Department of Energy 2013. http://dx.doi.org/10.3334/CDIAC/00001_V2013.

[5] Yang G, Ma S, Wang T, et al. Assessing the wind energy potential of China in considering its variability/ intermittency. Energy Conversion and Management 2020;113580. http://dx.doi.org/10.1016/j.enconman.2020.113580

[6] Liu F, Sun F, Liu W, et al. On wind speed pattern and energy potential in China. Applied Energy 2019;236:867-876.http://dx.doi.org/10.1016/j.apenergy.2018.12.056

[7] Chang R, Zhu R, Badger M, Hasager CB, Zhou R, Ye D, Zhang X. Applicability of synthetic aperture radar wind retrievals on offshore wind resources assessment in Hangzhou bay. China Energ 2014;7:3339-3354. http://dx.doi.org/10.3390/en7053339

[8] Chang R, Zhu R, Badger M, Hasager CB, Xing X, Jiang Y. Offshore wind resources assessment from multiple satellite data and WRF modeling over South China Sea. Rem Sens 2015;7:467-487. https://dx.doi.org/10.3390/rs70100467

[9] Zhang D, Li W, Lin Y. Wave energy in China: current status and perspectives. Renew Energy 2009;34:2089-2092. https://dx.doi.org/10.1016/j.renene.2009.03.014

[10] Xiao Z. China's Wind Power Resource Evaluation Report. China Meteoological Press 2009

[11] Hong L, Möller B. Offshore wind energy potential in China: under technical, spatial and economic constraints. Energy 2011;36:4482-4491. https://dx.doi.org/10.1016/j.energy.2011.03.071

[12] Li D, Geyer B, Bisling P. A model-based climatology analysis of wind power resources at 100-m height over the Bohai sea and the Yellow sea. Appl Energy 2016;179:575-589. https://dx.doi.org/10.1016/j.apenergy.2016.07.010

[13] Nie B, Li J. Technical potential assessment of offshore wind energy over shallow continent shelf along China coast. Renew Energy 2018;128:391-399. https://dx.doi.org/10.1016/j.renene. 2018.05.081

[14] Liang B, Liu X, Li H, Wu Y, Lee D. Wave climate hindcasts for the Bohai sea, Yellow sea, and East China sea. J Coast Res 2014a;32:172–180. https://dx.doi.org/10.2112/JCOASTRES-D-14-00017.1

[15] Lv X, Yuan D, Ma X, Tao J. Wave characteristics analysis in Bohai Sea based on ECMWF wind field. Ocean Eng 2014;91:159–171. https://dx.doi.org/10.1016/j.oceaneng.2014.09.010

[16] Li J, Chen Y, Pan S, Pan Y, Fang J, Sowa DM. Estimation of mean and extreme waves in the East China Seas. Appl Ocean Res 2016a;56:35–47. https://dx.doi.org/10.1016/j.apor.2016.01. 005

[17] Li J, Pan S, Chen Y, Fan Y, Pan Y. Numerical estimation of extreme waves and surges over the northwest Pacific Ocean. Ocean Eng 2018;153:225-241. https://doi.org/10.1016/j. oceaneng.2018.01.076

[18] Liang B, Fan F, Liu F, Gao S, Zuo H. 22-year wave energy hindcast for the china east adjacent seas. Renew Energy 2014b:71:200-207. https://doi.org/10.1016/j.renene.2014.05.027

[19] Wang Z, Dong S, Li X, Soares CG. Assessments of wave energy in the bohai sea, china. Renew Energy 2016;90:145-156. https://doi.org/10.1016/j.renene.2015.12.060

[20] Wu S, Liu C, Chen X. Offshore wave energy resource assessment in the east china sea. Renew Energy 2015;76:628-636. https://doi.org/10.1016/j.renene.2014.11.054

[21] Zheng C, Xiao Z, Peng Y, Li C, Du Z. Rezoning global offshore wind energy resources. Renew Energy 2018;129:1-11. https://doi.org/10.1016/j.renene.2018.05.090

[22] Bosch J, Staffell I, Hawkes AD. Temporally-explicit and spatially-resolved global onshore wind energy potentials. Energy 2017;131:207-217. https://doi.org/10.1016/j.energy.2017.05.052

[23] Zheng C. Dynamic self-adjusting classification for global wave energy resources under different requirements. Energy 2021;236:121525. https://doi.org/10.1016/j.energy.2021.12152

[24] Guedes Soares C, Bento AR, Goncalves M, Silva D, Martinho P. Numerical evaluation of the wave energy resource along the Atlantic European coast. Comput Geosci 2014;71:37-49. https://doi.org/10.1016/j.cageo.2014.03.008

[25] Gonçalves M, Martinho P, Guedes Soares C. Wave energy conditions in the western French coast. Renew Energy 2014;62:155-163. https://doi.org/10.1016/j.renene.2013.06.028

[26] Reeve DE, Chen Y, Pan S, Magar V, Simmonds DJ, Zacharioudaki A. An investigation of

the impacts of climate change on wave energy generation: The Wave Hub. Cornwall. UK. Renew Energy 2011;36:2404-2413. https://doi.org/10.1016/j.renene.2011.02.020

[27] Defne Z, Haas KA, Fritz HM. Wave power potential along the Atlantic coast of the southeastern USA. Renew Energy 2009;34:2197-2205. https://doi.org/10.1016/j.renene.2009.02.019

[28] Behrens S, Hayward J, Hemer M, Osman P. Assessing the wave energy converter potential for Australian coastal regions. Renew Energy 2012;43:210-217. https://doi.org/10.1016/j.renene. 2011.11.031

[29] Kim G, Jeong WM, Lee KS, Jun K, Lee ME. Offshore and nearshore wave energy assessment around the Korean Peninsula. Energy 2011;36:1460-1469. https://doi.org/10.1016/ j.energy. 2011.01.023

[30] Saenz-Aguirre A, Saenz J, Ulazia A, Ibarra-Berastegui G. Optimal strategies of deployment of far offshore co-located wind-wave energy farms. Energy Conv Mana 2022;251:114914. https:// doi.org/10.1016 /j.enconman.2021.114914

[31] Rusu E, Onea F. A parallel evaluation of the wind and wave energy resources along the Latin American and European coastal environments. Renew Energy 2019;143:1594-1607. https://doi.org/10.1016/j.renene.2019.05.117

[32] Lira-Loarca A, Ferrari F, Mazzino A, Besio G. Future wind and wave energy resources and exploitability in the Mediterranean Sea by 2100. Appl Energy 2021;302:117492. https://doi.org/ 10.1016/j.apenergy.2021.1

[33] Ferrari F, Besio G, Cassola F, Mazzino A. Optimized wind and wave energy resource assessment and offshore exploitability in the Mediterranean Sea. Energy 2020;190:116447. https://doi.org/10.1016/j.energy.2019.116447

[34] Haces-Fernandez F, Li H, Ramirez D. A layout optimization method based on wave wake preprocessing concept for wave-wind hybrid energy farms. Energy Conv Mana 2021;244:114469. https://doi.org/10.1016/j.enconman.2021.114469

[35] Wang Z, Duan C, Dong S. Long-term wind and wave energy resource assessment in the South China sea based on 30-year hindcast data. Ocean Eng 2018;163:58-75. https://doi.org/ 10.1016/j.oceaneng.2018.05.070

[36] Zheng C, Pan J, Li J. Assessing the China Sea wind energy and wave energy resources from 1988 to 2009. Ocean Eng 2013;65:39-48. https://doi.org/10.1016/j.oceaneng. 2013.03.006

[37] Zheng C, Li C. Variation of the wave energy and significant wave height in the china sea and adjacent waters. Renew Sustain Energy Rev 2015;43:381-387. https://doi.org/10.1016/j.rser. 2014.11.001

[38] Wen Y, Kamranzad B, Lin P. Joint exploitation potential of offshore wind and wave energy along the south and southeast coasts of China. Energy 2022;249:123710. https://doi.org/10.1016/ j.energy.2022.123710

[39] Wan Y, Zheng C, Li L, Dai Y, Zhang X. Wave energy assessment related to wave energy convertors in the coastal waters of china. Energy 2020;202:11774. https://doi.org/10.1016/j. energy.2020.117741

[40] Lin Y, Dong S, Wang Z, Soares CG. Wave energy assessment in the china adjacent seas on the basis of a 20-year swan simulation with unstructured grids Renew Energy 2019;136:275-295. https://doi.org/10.1016/j.renene.2019.01.01

[41] Li J, Pan S, Chen Y, Pan Y. Assessment of Tropical Cyclones in ECMWF Reanalysis Data over Northwest Pacific Ocean, 27th International Ocean and Polar Engineering Conference. San Francisco, California, USA. International Society of Offshore and Polar Engineers 2017

[42] Wen F. Developments and Characteristics of Offshore Wind Farms in China. Adv New Renew Energy 2016;4:152-158. (in Chinese)

[43] Jourdain NC, Barnier B, Ferry N, Vialard J, Menkes CE, Lengaigne M, Parent L. Tropical cyclones in two atmospheric (re) analyses and their response in two oceanic reanalyses. Ocean Model 2014;73:108–122. https://doi.org/10.1016/j.ocemod.2013.10.007

[44] Li J, Chen Y, Pan S. Modelling of extreme wave climate in China seas. J Coast Res 2016b;75:522–526. https://doi.org/10.2112/SI75-105.1

[45] Jelesnianski P. A numerical calculation of storm tides induced by a tropical storm impinging on a continental shelf. Mon Weather Rev 1965;93:343. https://doi.org/10.1175/1520-0493(1993) 093<0343:ANCOS>2.3.CO;2

[46] Pan Y, Chen Y, Li J, Ding X. Improvement of wind field hindcasts for tropical cyclones.

Water Sci Eng 2016;9:58-66. https://doi.org/10.1016/j.wse.2016.02.002

[47] Qi J, Chen C, Beardsley RC, Perrie W, Cowles GW, Lai Z. An unstructured-grid finite-volume surface wave model (FVCOM-SWAVE): implementation, validations and applications. Ocean Model 2009;28:153-166. https://doi.org/10.1016/j.ocemod.2009.01.007

[48] Ozger M, Altunkaynak A, Sen Z. Stochastic wave energy calculation formulation. Renew Energy 2004;29:1747-1756. https://doi.org/10.1016/j.renene.2004.01.009

[49] Hasselmann K, Barnett TP, Bouws E, et al. Measurements of wind-wave growth and swell decay during the joint North Sea wave project (JONSWAP). Deat Hydrogr Zeit 1973;12. https://doi.org/10.1093/ije/27.2.335

[50] Wan Y, Zheng C, Li L, Dai Y, Zhang X. Wave energy assessment related to wave energy convertors in the coastal waters of china. Energy 2020;202:117741. https://doi.org/10.1016/j.energy.2020.117741

[51] Ying M, Zhang W, Yu H, Lu X, Feng J, Fan Y, Zhu Y, Chen D. An overview of the china meteorological administration tropical cyclone database. J Atmos Ocean Technol 2014;31:287-301. https://doi.org/10.1175/JTECH-D-12-00119.1

[52] https://en.wind-turbine-models.com

[53] Yang F, Zhang X, Chen S, Wang Z. The Development and Operation of Offshore Wind Farms in China. Proceedings of the 2015 Asia-Pacific Energy Equipment Engineering Research Conference 2015.